PRAMANA
— journal of
physics

© Indian Academy of Sciences

Vol. 74, No. 2
February 2010
pp. 247–259

Design studies of a high-current radiofrequency quadrupole for accelerator-driven systems programme

S V L S RAO* and P SINGH
Nuclear Physics Division, Bhabha Atomic Research Centre, Mumbai 400 085, India
*Corresponding author. E-mail: giri_786@rediffmail.com

MS received 3 August 2009; revised 7 October 2009; accepted 9 October 2009

Abstract. A 3 MeV, 30 mA radiofrequency quadrupole (RFQ) accelerator has been designed for the low-energy high-intensity proton accelerator (LEHIPA) project at BARC, India. The beam and cavity dynamics studies were performed using the computer codes LIDOS, TOUTATIS, SUPERFISH and CST microwave studio. We have followed the conventional design technique with slight modifications and compared that with the equipartitioned (EP) type of design. The sensitivity of the RFQ to the variation of input beam Twiss–Courant parameters and emittance has also been studied. In this article we discuss both design strategies and the details of the 3D cavity simulation studies.

Keywords. Radiofrequency quadrupole; emittance; Twiss parameters; beam transmission; equipartioning; low-energy high-intensity proton accelerator; cavity dynamics.

PACS Nos 29.27.-a; 29.27.eg; 29.27.Fh; 41.75.-i

1. Introduction

Radiofrequency quadrupole (RFQ) [1–4] accelerators are extensively used as injectors in the high-current Linacs because of their remarkable capability of simultaneously focussing, bunching and accelerating the low-energy ion beams with high transmission (>90%) and minimum beam emittance growth. However, in any RF accelerator the beam must be longitudinally bunched so that all particles will be accelerated. In a conventional accelerator such as the drift tube Linac (DTL), bunching is accomplished prior to injection into the Linac using one or more RF bunching cavities. In buncher cavities RF eletric fields are applied to the DC input beam to produce a velocity modulation in which early particles are decelerated and late particles are accelerated. After a suitable drift space, the beam becomes bunched, ready for injection into the Linac. The bunching is usually not very efficient, especially for high-current beams because of the higher space-charge forces at low energies. In high-intensity beams, the bunching process causes an increase in the beam density, which increases the space-charge forces and often results in a

blow-up of the transverse beam emittance. These are the fundamental limitations of conventional Linacs like DTL. However, the RFQ eliminates these problems by employing the adiabatic bunching process. This process increases the capture efficiency of the RFQ to nearly 100%. Because of their high capture efficiency at low energies, the RFQs suite well as a first unit of high-current RF linear accelerators in many advanced applications, such as production of radioactive ion beams [5,6], accelerator-driven systems (ADS) [7] for effective utilization of thorium resources and spallation neutron source (SNS) [8].

In view of the importance of accelerator-driven system (ADS), the R&D activity for the design and development of a 20 MeV, 30 mA CW proton accelerator (LEHIPA) as an injector to 1 GeV Linac has been initiated in BARC, India. The LEHIPA [9] mainly consists of a 50 keV ECR ion source, low energy beam transport (LEBT) line, 3 MeV radiofrequency quadrupole (RFQ) accelerator, medium energy beam transport (MEBT) line and a 20 MeV drift tube Linac (DTL).

The beam dynamics of RFQ Linacs have been extensively studied by LANL [10] and a generalized method was proposed, where RFQ was divided into four sections, namely, radial matching (RM), shaper (SH), gentle buncher (GB) and accelerator (AC) sections. In this generalized method, the focussing factor (B) and vane voltage (V) are kept consant all along the RFQ. Several design methods have been proposed by Yan *et al* [11,12], Chuan Zhang *et al* [13] and Jameson [14,15] for minimizing the emittance growth and the resulting beam losses. We have used two different methods (generalized or conventional method with slight modifications and EP method) and made detailed studies for the design of our RFQ. The details of these studies are discussed in the following sections.

2. Design strategy

2.1 *Conventional design*

In the conventional design, the RFQ is divided into four sections: RM, SH, GB and AC. In the GB section, the spatial bunch length (Z_{b}) and zero current phase advances in transverse and longitudinal directions ($\sigma_{0\mathrm{t}}$, $\sigma_{0\mathrm{l}}$) are kept constant. These conditions lead to the constant space charge and external forces while bunching and accelerating the beam in the GB section. The structure parameters like modulation (m) and aperture (a_p) in the GB section are generated by solving eqs (1)–(3) which result from the above conditions.

$$\beta\psi = \text{const.}, \tag{1}$$

$$\frac{AV\sin(\phi_{\mathrm{s}})}{\beta^2} = \text{const.}, \tag{2}$$

$$\frac{V\chi}{a_p^2} = \text{const.}, \tag{3}$$

where ψ and $a_p/\sqrt{\chi}$ are the phase width of the separatrix and average aperture radius (r_0).

In the AC section, the acceleration efficiency (A) and modulation (m) are kept constant at values equal to those at the end of GB. In the SH section, the synchronous phase (ϕ_s) and modulation (m) are linearly ramped from -90° and 1 to the values at the beginning of the GB.

2.2 *Equipartitioned design*

An equipartitioned (EP) beam [16–19] has equal transverse and longitudinal temperatures ($T_l = T_t$). For a matched bunch in a smooth-focussing system, the temperatures can be related to the r.m.s. beam widths and normalized r.m.s. emittances as

$$\frac{T_l}{T_t} = \frac{\varepsilon_{ln}^2}{\varepsilon_{tn}^2}\frac{a^2}{(\gamma b)^2}, \tag{4}$$

where $\varepsilon_{tn}, \varepsilon_{ln}$ are full (100%) normalized emittances of the uniform ellipsoidal beam distribution. Here a and b denote the transverse and longitudinal beam sizes. From the envelope equations, the full current phase advances (σ_t, σ_l) are given by

$$\sigma_t = \frac{\varepsilon_{tn}\lambda}{a^2\gamma}, \tag{5}$$

$$\sigma_l = \frac{\varepsilon_{ln}\lambda}{b^2\gamma^3}, \tag{6}$$

where λ is the RF wavelength and γ is the relativistic factor.

The full current phase advances for a uniform ellipsoidal beam distribution are also related to the external focussing forces as

$$\sigma_t^2 = \sigma_{0t}^2 - \frac{3Z_0 I\lambda^3(1-f)}{8\pi m_0 c^2 a^2 b\gamma^3}, \tag{7}$$

$$\sigma_l^2 = \sigma_{0l}^2 - \frac{3Z_0 I\lambda^3 f}{4\pi m_0 c^2 a^2 b\gamma^3}, \tag{8}$$

where $Z_0 = 377\ \Omega$ and form factor (f) is a function of $\gamma b/a$. When $0.85 \le \gamma b/a \le 5$ then $f = a/3\gamma b$.

In order to have the EP beam $\varepsilon_{ln}/\varepsilon_{tn} = \gamma b/a$. By choosing the EP ratio, $\varepsilon_{ln}/\varepsilon_{tn}$, we can calculate the beam radii as a function of external forces (σ_{0t}, σ_{0l}). The phase advances are chosen based on the following constaints in order to avoid envelope instabilities [20], resonances and space-charge limits

$$\sigma_{0t}, \sigma_{0l} \le 90^\circ \tag{9}$$

$$\frac{\sigma_{\mathrm{t}}}{\sigma_{\mathrm{l}}} \neq n, \frac{1}{n} (\text{where } n \text{ is an integer}) \tag{10}$$

$$\frac{\sigma_{\mathrm{l}}}{\sigma_{0\mathrm{l}}}, \ \frac{\sigma_{\mathrm{t}}}{\sigma_{0\mathrm{t}}} > 0.4. \tag{11}$$

By choosing the values of $\sigma_{0\mathrm{t}}$, $\sigma_{0\mathrm{l}}$ and the vane voltage (V), one can calculate all the structure parameters using simple analytical formulae given in ref. [21].

3. Calculation of structure parameters for EP design

By choosing the values of $\sigma_{0\mathrm{t}}$ and $\sigma_{0\mathrm{l}}$ as a function of the velocity of the synchronous particle (β_{s}), we can calculate the focussing factor (B) from the given equation.

$$\mathbf{B} = 2\pi\sqrt{2\sigma_{0\mathrm{t}}^2 + \sigma_{0\mathrm{l}}^2}. \tag{12}$$

The vane voltage has been chosen by keeping the peak surface field (E_{s}) less than 1.8 times the Kilpatric field [22] (<33 MV/m at 352.21 MHz) in order to avoid sparking

$$\mathbf{Es} = \frac{\kappa V}{r_0}, \tag{13}$$

where κ is the field enhancement factor [23], which depends on ρ_{t}/r_0, modulation (m) and L/r_0, where ρ_{t} and L are the transverse radius of curvature and cell length ($\beta_{\mathrm{s}}\lambda/2$) respectively.

The focussing factor (B) is related to the vane voltage (V) and the structure parameters, m and a_p, as shown in the following equations given in ref. [3]:

$$\mathbf{B} = \frac{qV\lambda^2}{m_0c^2r_0^2} \tag{14}$$

$$r_0 = \frac{a_p}{\sqrt{\chi}} \tag{15}$$

$$\sigma_{0\mathrm{l}} = \sqrt{\frac{\pi^2 AV\sin(\phi_{\mathrm{s}})}{m_0c^2\beta_{\mathrm{s}}^2}} \tag{16}$$

$$A = \frac{m^2 - 1}{m^2 I_0(2\pi a_p/\beta_{\mathrm{s}}\lambda) + I_0(2\pi m a_p/\beta_{\mathrm{s}}\lambda)} \tag{17}$$

$$\chi = 1 - AI_0\left(\frac{2\pi a_p}{\beta_{\mathrm{s}}\lambda}\right). \tag{18}$$

By choosing $\sigma_{0\mathrm{t}}$, $\sigma_{0\mathrm{l}}$, E_{s} and ϕ_{s} as a function of β_{s}, one can calculate the structure parameters m and a_p and the required vane voltage (V) using the above equations. In EP design one can keep the vane voltage constant and see whether the maximum E_{s} is within 33 MV/m in order to avoid sparking or else one can keep E_{s} constant at a value below 33 MV/m and calculate the required vane voltage. In our EP design, we have chosen constant E_{s} and calculated the vane voltage along the RFQ.

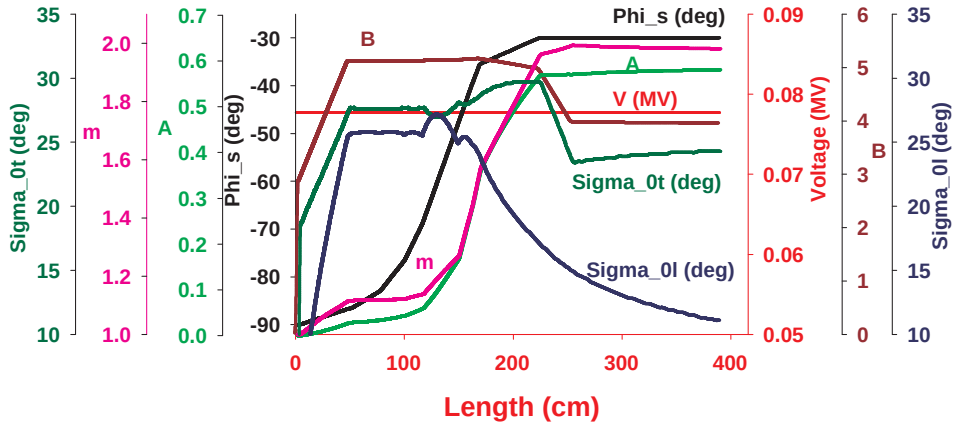

Figure 1. RFQ parameters along the length for design D1.

4. Simulation studies

The beam dynamics has been done using the computer codes LIDOS [24] and TOUTATIS [25]. We had studied two different designs for our RFQ, based on the conventional method (D1) and EP (D2).

4.1 *Design (D1)*

In this design we have made some modifications in SH and AC sections of the RFQ, in order to reduce the concentration of the beam loss in a small region. In the SH section the focussing factor (B) is increased from a lower value at the input to the maximum, kept constant at the maximum value in the GB section and again reduced in the AC section. A lower value of B at the beginning of the SH section of the RFQ is prefered since it reduces the space-charge effects at the injection which is very important for high-current RFQ. This leads to achieve a good input match. The lower value of B at the end of the RFQ allows the current independent matching of the beam to the subsequent accelerating structures (DTL).

In the conventional design, where B is kept constant in the entire RFQ, the maximum beam loss takes place at the end of the GB section where the aperture is minimum. With the variation of B as shown in figure 1, the beam loss is not confined to a small region, rather it is distributed along the RFQ.

4.2 *EP design (D2)*

The overall length of the RFQ will depend mainly on the choice of EP ratio. In this design, we have taken the EP ratio to be 1.44 and chosen the value of σ_{0t} and σ_{0l} as a function of β_s based on the constraints discussed in §2.2. We have varied B and vane voltage (V) to keep the peak surface field E_s a constant at 32 MV/m

Table 1. Parameters of the RFQ.

Parameter	D1	D2	Unit
Ion species	H^+	H^+	Proton
Frequency	352.21	352.21	MHz
I/P energy	0.05	0.055	MeV
O/P energy	3.00	3.000	MeV
Beam current	30.00	30.000	mA
I/P Norm. r.m.s. emittance	0.02	0.02	π cm-mrad
Vane voltage	77.7	69–135	kV
Peak field	32.89	32.83	MV/m
Number of particles	50,000	50,000	Particles
Transmission	99.24	99.66	%
Accelerated	99.17	99.4	%
Modulation	1.99	1.99	
Focussing factor	3–5.2	6.23–3.43	
Max E_z field	2.13	2.27	MV/m
Length	3.98	4.15	m

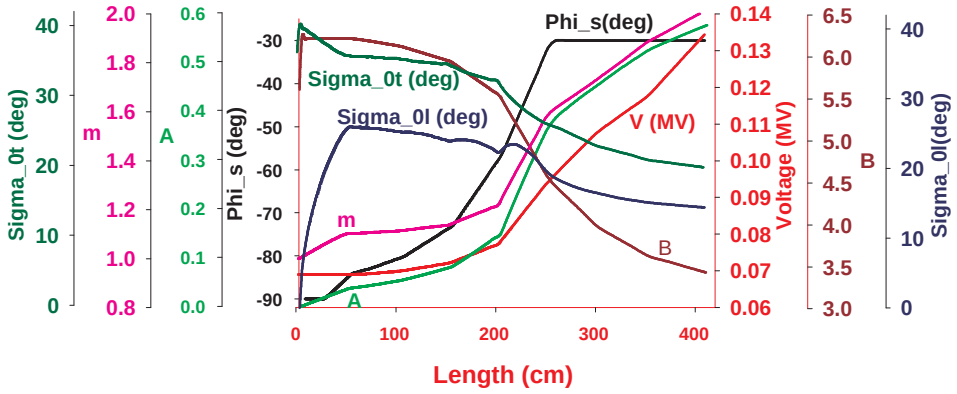

Figure 2. RFQ parameters along the length for design D2.

all along the RFQ. In order to bring the overall length of the RFQ to around 4 m as in design D1, we have slightly increased the input energy of the beam to 55 keV.

4.3 *Simulation results*

The input and output parameters of the RFQ are listed in table 1.

The variations of different parameters along the length of the RFQ for both designs are shown in figures 1 and 2.

The transmission and the power deposited (in Watts) due to beam loss along the length of the RFQ for the designs D1 and D2 are shown in figures 3 and 4 respectively.

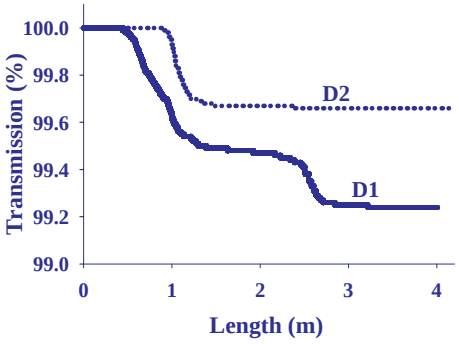

Figure 3. Transmission along the RFQ length for D1 and D2.

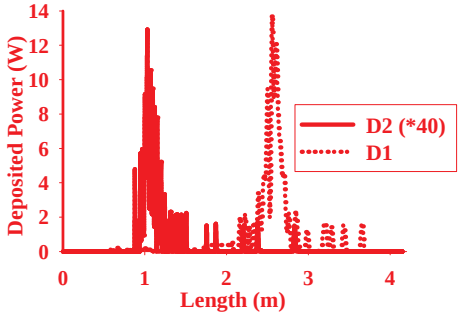

Figure 4. Power deposited due to beam loss along the RFQ length for D1 and D2.

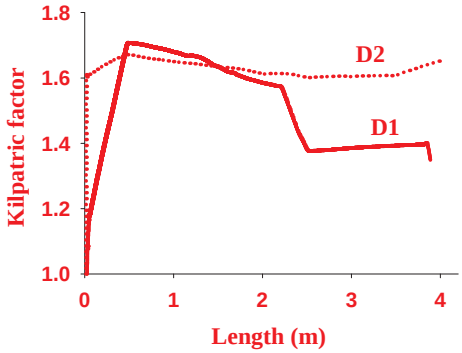

Figure 5. Kilpatric factor for design D1 and D2 along the RFQ length.

The variation of the Kilpatric factor along the RFQ length for both D1 and D2 is shown in figure 5. In D2, the Kilpatric factor was kept almost constant in the entire RFQ and as a result there is ramping of the vane voltage.

The variation of the normalized r.m.s. emittance for both D1 and D2 is shown in figure 6.

It is clearly seen that the power deposited due to beam loss (<0.3 W) and emittance growth (∼5%) are less in design D2, when compared to D1 ((>10 W) and (∼10%)). So, the design D2 is favourable from the beam dynamics point of view.

5. 2D cavity design

The 2D cavity design has been done using the computer code SUPERFISH [26]. Since the focussing factor (B) is varied along the length for both D1 and D2 designs, r_0 and also power dissipation vary along the length of the RFQ. The variation of the power dissipation along the RFQ length for both D1 and D2 is shown in figure 7. The total power loss in one quadrant of the RFQ can be calculated as the area under the curve in figure 7. The power dissipation in the RFQ structure for D2

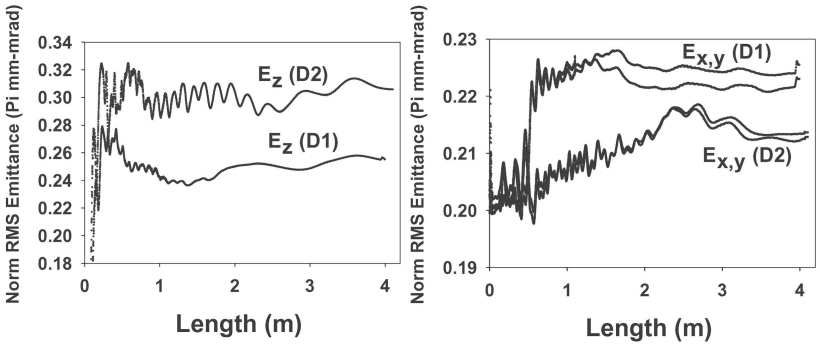

Figure 6. Variation of normalized r.m.s. emittance for D1 and D2 along the RFQ length.

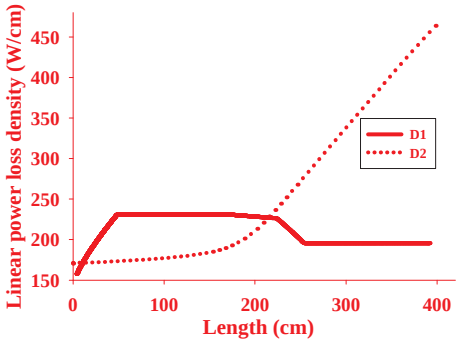

Figure 7. Linear power loss density (W/cm) along the length of RFQ.

Table 2. RF parameters of cavity.

Parameter	Value	Unit
Quadrupole mode	352.21	MHz
Quality factor (Q_0)	7600	
Beam power	88.5	kW
Cu power (1.3 ∗ SF)	432.5	kW
Total RF power (1.3 ∗ SF)	521	kW
Mode separation	10.11	MHz

design is almost twice, when compared to D1 design. Since the length of the RFQ is almost same for both the designs, the power loss density is more for design D2. Since the required RF power is much larger in design D2, D1 has an advantage and has been chosen for fabrication. The RF parameters of the RFQ cavity based on the design D1 is shown in table 2, where SF is the power calculated using SUPERFISH program. The detailed 3D design and the sensitivity analysis have therefore been done for design D1.

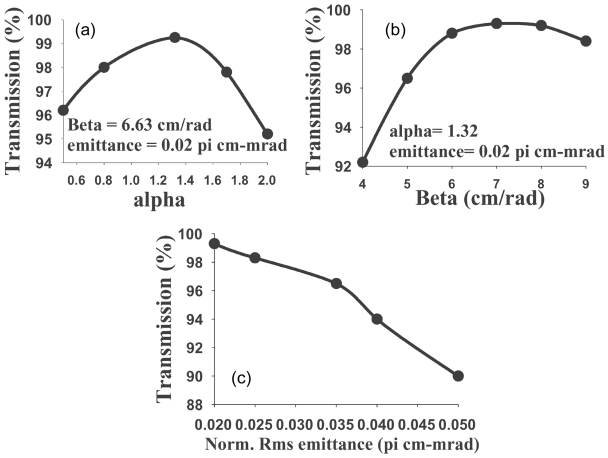

Figure 8. Variation of transmission with input (**a**) α, (**b**) β and (**c**) ε_{t}.

6. Sensitivity analysis

We have studied the dependence of the transmission of the RFQ as a function of the input beam Twiss–Courant parameters (α, β) and emittance $(\varepsilon_{\mathrm{t}})$. This is shown in figure 8. It is clear from the analysis that the transmission is more sensitive to the input parameter α (i.e. orientation) of the beam ellipse.

7. 3D cavity simulations

To study the effects of the asymmetric features like beginning cell (BC), end cell (EC) and coupling cell (CC) of the RFQ, complete 3D electromagnetic simulations are needed. The computer code SUPERFISH is a two-dimensional code, which cannot be used for structures that are asymmetric, or having asymmetric features. We have used the computer code CST Microwave studio [27] for the complete 3D cavity design. The effects of BC, EC and CC on the quadrupole mode frequencies are extensively studied using transfer matrix theory [28,29].

7.1 *BC and EC designs*

At both ends of an RFQ, undercuts must be performed in the vanes in order to close the magnetic field lines. The vane undercut causes a local mismatch and an unwanted frequency shift. The schematic of the vane undercut is shown in figure 9. In order to tune the BC and EC to the required quadrupolar cross-sectional frequency (f_{Q2d}) the undercut depth (d) and the thickness (t) are varied. The optimized parameters of BC and EC are shown in table 3. In order to reduce the computational time, we have modelled only 6.4 cm and 10 cm for BC and EC respectively. A resonant cavity made by different elements (like main body and the

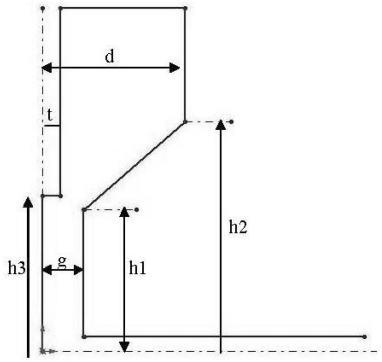

Figure 9. Schematic of the vane undercut.

Table 3. Parameters of BC and EC.

Parameters	BC	EC
Height (h1)	4 cm	3.8 cm
Height (h2)	6 cm	6 cm
Vane gap (g)	0.875 cm	1.037 cm
Depth (d)	4.4 cm	5.392 cm
Height (h3)	4.5 cm	4.8 cm
Thickness (t)	0.16 cm	0.23 cm

end cells) having slightly different resonant frequencies, will resonate at a frequency obtained by averaging the single element frequencies, weighted by the amount of energy stored in each element [30,31]. If the resonant frequencies of the BC, EC and ideal RFQ cavities are f_{BC}, f_{EC} and f_{Q2d} then the frequencies of the real RFQ (with beginning and end cells) is given by

$$f_{\mathrm{realRFQ}} \sim \frac{f_{\mathrm{BC}} l_{\mathrm{BC}} + f_{\mathrm{Q2dRFQ}} l_{\mathrm{RFQ}} + f_{\mathrm{EC}} l_{\mathrm{EC}}}{L}. \tag{19}$$

If BC and EC are tuned exactly to f_{Q2d}, then the RFQ with undercuts will resonate at f_{Q2d}. Moreover, the dipole mode frequency for the RFQ with undercuts increases and comes closer to the quadrupole mode frequency, since undercuts are tuned to the quadrupole mode. The dipole mode frequency for the ideal RFQ (f_{d2d}) without undercuts (i.e., open at both ends) is 342.1 MHz and it was observed from the simulations that the dipole mode frequency for the real RFQ (f_{d}) with undercuts was 345.2 MHz.

7.2 *Coupling cell design*

A single segment of 4 m long RFQ will be very unstable because the longitudinal higher-order modes (HOMs) are very close in frequency from the accelerating mode. The cavity was therefore split into two 2-m-long segments, and followed the LEDA

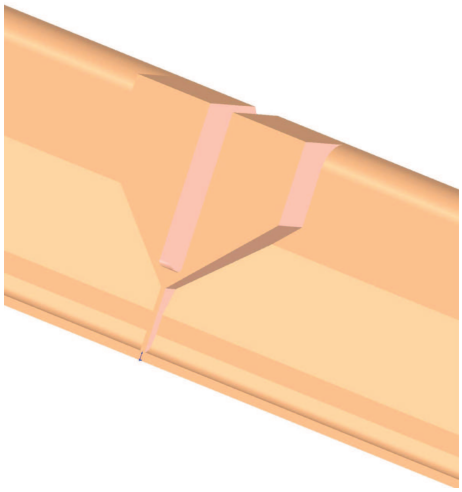

Figure 10. Schematic of the coupling cell.

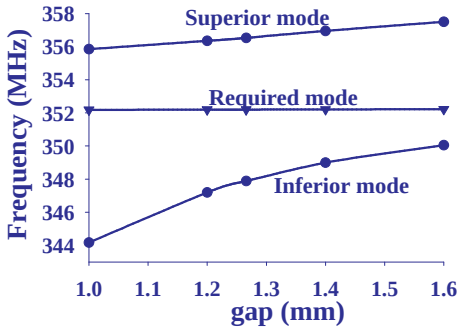

Figure 11. Variation of mode frequencies with gap.

resonant coupling technique [32]. The principle is to make the structure insensitive to the perturbations, which is similar to the $\pi/2$ structure in coupled cavity Linacs (CCL), in which the inferior and superior modes are equally spaced in frequency from the operating mode. To design the CC gap [33], the 4-m-long RFQ with a symmetry exactly at the centre of the CC gap was modelled. The schematic of the coupling cell (CC) is shown in figure 10.

The variation of the mode frequencies with gap is shown in figure 11. It was observed that the inferior and superior modes are separated equally from the operating mode for a gap of 1.3 mm. The cell parameters have therefore been optimized with a gap value of 1.3 mm.

8. Summary

We have designed a 3 MeV, 30 mA RFQ using two different methods (conventional and EP). It is seen from the beam dynamics studies that in design D2 (EP) the

power deposited due to beam loss and emittance growth is less, whereas from the cavity simulation results, the design D1 (conventional) is preferable, since the RF power dissipation is almost half when compared to D2. From the fabrication point of view also the design D1 is preferable since ρ_t is constant. Therefore, we have planned to follow the design D1 for the fabrication of a prototype RFQ and the detailed sensitivity analysis and 3D simulations of the cavity have been done for this design (D1). Based on these studies the fabrication of prototype RFQ have been started.

Acknowledgements

The authors thank Drs V C Sahni, S Kailas and R K Choudhury for their keen interest in the project. They also thank Dr R Duperrier for providing the TOUTATIS code and Rajni Pande and Shweta Roy for fruitful discussions.

References

[1] I M Kapchinskiy and V A Tepliakov, *Prib. Tekh. Eksp.* **2**, 19 (1970)
[2] John W Staples, *AIP Conf. Proc.* **249**, 1483 (1992)
[3] M Weiss, Radiofrequency quadrupole, *Proc. CAS* (Aarhus, Denmark, 1986); CERN 87-10 (1987)
[4] A Schempp, *Radiofrequency quadrupole*, CERN-92-03, 1992, p. 522
[5] J Vervier (GANIL): EURISOL, Preliminary design study of the next-generation European ISOL radioactive nuclear beam facility, Contract Number HPRI-1999-CT-50001
[6] A Chakrabarti, *J. Nucl. Particle Phys.* **24**, 1361 (1998)
[7] H Nifenecker, O Maplan and S David, Accelerator-driven subcritical reactors, Institute of Physics, *Series in fundamental and applied nuclear physics*
[8] National Spallation Neutron Source, NSNS/CDR-2/VI, May 1997
[9] P Singh, *Status of the LEHIPA project at BARC*, InPAC-2006, p. 50
[10] K R Crandall, R H Stokes and T P Wangler, RF Quadrupole beam dynamics design studies, *Proceedings of 1979 Linear Accelerator Conference* (Brookhaven National Laboratory, Upton, NY, 1980), BNL-51134, p. 205; *LANL Manual of RFQ design codes* (Los Alamos National Laboratory Report LA-UR-96-1836 (revised February 12, 1997)
[11] X Q Yan *et al*, *Nucl. Instrum. Methods in Phys. Res.* **A554**, 132 (2005)
[12] X Q Yan *et al*, *Nucl. Instrum. Methods in Phys. Res.* **A577**, 402 (2007)
[13] Chuan Zhang *et al*, *Nucl. Instrum. Methods in Phys. Res.* **A586**, 153 (2008)
[14] R A Jameson *et al*, *Scaling and optimization in high-intensity linear accelerators*, LA-CP-91-272, Los Alamos National Laboratory, July 1991 (introduction of LINACS design code)
[15] R A Jameson, An approach to fundamental study of beam loss minimization, edited by Y K Batygin, *AIP Conference Proceedings* 480, Space Charge Dominated Beam Physics for Heavy Ion Fusion, Saitama, Japan, 1998
[16] T P Wangler, *Principles of RF linear accelerators* (Wiley, New York, 1998)
[17] R A Jameson, *IEEE Trans. Nucl. Sci.* **NS-28**, 2408 (1981)
[18] I Hofmann, Equipartitioning and halo due to anisotropy, *Proc. 1997 Part. Accel. Conf.*

[19] I Hofmann *et al*, *Review of beam dynamics and space charge resonances in high intensity Linacs*, EPAC 2002
[20] M Reiser, *Theory and design of charged particle beams* (John Wiley & Sons, New York, 1994)
[21] Jean-Michel Lagniel, Tools for the design of high-current Linacs, *Proc. 1994 Linac Conf.* (Tsukuba, Japan)
[22] W D Kilpatrick, *A criterion for vacuum sparking design both RF and DC*, Radiation Lab Report UCRL-2321 (1953)
[23] K R Crandall, *Effects of vane-tip geometry on the electric fields in radiofrequency quadrupole Linacs*, Los Alamos National Laboratory Report, LA-9695-MS, April 1983
[24] LIDOS, A Computer Code for Beam Dynamics of RFQ Linac, Version 1.1
[25] R Duperrier and R Ferdinand, Toutatis, The CEA-Saclay RFQ Code, *XX International Linac Conference* (Monterey, CA, 2000)
[26] J H Billen and L M Young, Poisson Superfish, LA-UR-96-1834, LANL
[27] CST microwave studio, simulation tool for electromagnetic analysis and design, CST, Germany
[28] A Palmieri and A Pisent, Perturbation analysis of couple RFQs, Internal Note, INFN
[29] Francesco Grespan, Stabilizzazione del campo accelerante nel quadrupolo a radiofrequenza del progetto SPES:Caratterizzazione teorica E risultati sperimetali, Universita Degli Studi di Padova
[30] J C Slater, *Microwave electronics* (Van Nostrand, New York, 1950) p. 81
[31] M Vretenar, RF cavities design codes and their application to the design of RFQs, CERN/PS 90-11 (RF-HI)
[32] J Browman *et al*, *Couple RFQs as compensated structures*, Linac90, Albuquerque, p. 70
[33] A Pisent, *Equivalent lumped circuit study for field stabilization of a long four-vanes RFQ*, Linac98, Chicago, p. 968